APPENDIX-II
Topography and Geology

THE STUDY ON SABO AND FLOOD CONTROL
FOR WESTERN RIVER BASINS OF MOUNT PINATUBO
IN THE REPUBLIC OF THE PHILIPPINES

FINAL REPORT

SUPPORTING REPORT

APPENDIX II TOPOGRAPHY AND GEOLOGY

Table of Contents

List of Tables

List of Figures

CHAPTER 1 TOPOGRAPHY

1.1 Topographic Condition in the Study Area

1.1.1 Topography

Figure 1.1.1 shows a topographic map of the study area. Mount Pinatubo is situated at an approximate latitude of 15°08'20" North and longitude of 120°21'35" East. Before June 1991, the elevation of Mount Pinatubo was 1,745 m above sea level. The surrounding mountains are older volcanic centers and relics of ancestral Mount Pinatubo. The gently-sloping apron consists of thick pyroclastic-flow and lahar (volcanic mudflow) deposits. The volcano is located at the boundary of the provinces of Zambales, Pampanga and Tarlac.

Mount Pinatubo is densely and deeply dissected by eight major river systems, each characterized by radial drainage and ending in broad, gently sloping aprons of laterally coalescing alluvial fans which extend beyond the flanks of the mountain. These major river systems are, clockwise from the North, the O'Donnell, Sacobia-Bamban, Abacan, Pasig-Potrero, Gumain, Sto. Tomas, Maloma and Bucao Rivers. Three rivers, namely Sto. Tomas, Maloma and Bucao Rivers, flow down the mountainous slopes of western Pinatubo into the South China Sea.

The western Pinatubo is different from eastern side in that non-volcanic mountains exist at the foot of western Mount Pinatubo such as Mount Iba, Mount Lunitan, Mount Maquineng and Mount Mabolinoc. These mountains determine the direction of the three river systems of west Pinatubo.

The Bucao River system flows north-west through the northernmost part of the western Pinatubo area. It travels west along the southern part of the Mount Iba range before joining the Balin Baquero River. After this confluence, it flows south of Botolan city to the South China Sea. The Balin Baquero River joins the Maraunot River, Lubao River and other tributaries at the east basin of the Mount Lunitan mountain range.

The Maloma River flows towards the south-east of the Mount Pinatubo mountain range and then flows down between the mountain ranges of Mount Lunitan and Mount Maquineng to the South China Sea.

The Sto. Tomas River flows down the mountain range of Mount Pinatubo towards the south (Marella River). At the confluence of the Mapanuepe River or at the foot of Mount Mabolinoc, the Sto. Tomas River changes direction to the west before flowing through the northern part of San Marcelino to the South China Sea.

1.1.2 Volcanic Activities

Mount Pinatubo is surrounded by a highly dissected depositional apron of older pyroclastic flow, lahar, and associated stream deposits. According to a geological survey by Philippine Institute of Volcanology and Seismology (PHIVOLCS) and US Geological Survey (USGS), older eruptive periods have been identified by ^{14}C dates on charcoal in pyroclastic flow deposits at about 2,500 to 3,000, 5,000 to 6,000 and 35,000 years before 2002. The last eruption has been dated at 460±30 years ago.

On July 16, 1990, an M7.8 earthquake occurred along the Philippine Fault, about 100 km northeast of Mount Pinatubo. The seismic records measured by PHIVOLCS show that an M4.8 earthquake occurred about 10 km southeast of Mount Pinatubo a few hours after the main shock. It was thought that the renewal of Mount Pinatubo activity may have been caused by an earthquake along the Digdig Fault, a segment of the Philippine Fault Zone, creating a landslide along the northwest side of the volcano.

The initial eruptive activity was characterized by minor steam and ash explosions 1.5 km northwest of the summit. Only a very thin layer of ash was deposited over the area and the surrounding forests near the explosion vents were devastated, however no lahars were observed. It was only after some major eruptive sequences on July 12 that the pyroclastic-fall and pyroclastic-flow deposits appeared on the flanks of the edifice.

On June 15, 1991, after 400-500 years of dormancy, Mount Pinatubo awoke with a climatic Plinian eruption. Mount Pinatubo's summit was lowered from 1,745 m to 1,449 m as shown in Figure 1.1.2. The caldera floor was partially filled with water to form a lake. The early filling may have been attributed partly to groundwater seepage while the rest could be due to rainfall and leakages of brine from the pre-volcanic basement.

1.1.3 Pyroclastic Fall and Flow Deposits

Areas within the 10-40 km radius danger zone of Mount Pinatubo bore the brunt of heavy ash fall blown all over the archipelago. The volume of the pyroclastic flow deposited on the slopes of Mount Pinatubo was estimated to be approximately 5 to 7 billion m^3. These hot deposits, up to 220 m thick in places, covered an area of approximately 120 km^2. They completely filled the upper catchment of the rivers and formed broad deposition surfaces that extended as far as 16 km downstream from the vent. The pyroclastic flow deposit, lahar deposit (as of 1991) and isopack line of ashfall are shown in Figure 1.1.3.

The total accumulation of pyroclastic flow deposits was the greatest to the west and northwest in the Bucao River, but substantial deposition also occurred to the southwest in the Marella River, to the east in the Sacobia-Bamban River, and to the north in the O'Donnell River. Figure 1.1.4 shows the deposition and erosion of pyroclastic material in the Marella River from 1991 to 2002.

1.1.4 Lahar

(1) Lahar Characteristics

"Lahar" is an Indonesian term, defined as "a rapidly flowing mixture of volcanic rock debris and water from a volcano". Lahars from Mount Pinatubo, triggered by heavy monsoon or typhoon rainfalls on erodible erupted materials, have been flowing into densely populated areas of Luzon Island since the eruption of June 1991. Although the toll of lives was small, enormous property loss and social disruption was caused. For the following four years (1991 – 1994), the most devastating lahars were generated during prolonged southwesterly monsoon rains that were induced by the passage of tropical typhoons in the vicinity of Luzon.

Lahars were classified into the following two types based on the flow characteristics:

1) Debris flows typically had peak discharges of several hundred to a thousand m^3/s and contained approximately 60-65% (rarely, 70%) sediment by volume.

2) Hyper concentrated flows typically had peak discharges of several hundred m^3/s and contained approximately 50% sediment by volume. Hyper concentrated flows are numerically more common, but the large debris flows carry a large part of the sediment that is deposited downstream.

(2) Grain Size Distribution

The grain sizes and specific gravity have a great influence on sediment transportation. Regardless of whether it originates as a primary hyper-concentrated flow or a debris flow, flows with hyper concentrations of sediments volumetrically dominated the flow system and depositional records in the

downstream reach.

Hyper-concentrated flow deposits in the eastern drainage of Mount Pinatubo are dominated by sand-size phenocrysts from the pyroclastic flow deposits with an admixture of mineral grains from older deposits as shown in Figure 1.1.5. Grain size in the western Pinatubo area is smaller than that in eastern area as shown in the figure. Pumice clasts are present but are volumetrically minor; most are preserved in coarse deposits near the surface.

1.1.5 River System

Figure 1.1.6 shows the boundary map of the three river basins, which was developed based on the aerial photographs taken in May 2002.

(1) Bucao River System

The Bucao River system consists mainly of the following sub-basins:

Bucao River System

River System	Sub-system	Tributary	Catchment Area (km^2)	Lahar Source
Bucao	Upper Bucao	Upper Bucao	142	Yes
		Balintawak	154	No
	Balin Baquero	Balin Baquero	153	Yes
		Lubao	51	Yes
		Maraunot	12	Yes
	Lower Bucao	Baquilan	61	No
	-	Others	82	
	TOTAL		655	

There are six major tributaries in the Bucao River system. Four of these tributaries are still identified as lahar sources. These are the Upper Bucao, Balin Baquero, Lubao and Maraunot Rivers. The total catchment area of these four tributaries is 358 km^2, which equates to 55% of the Bucao River system.

(2) Maloma River System

The followings are tributaries of the Maloma River System.

Maloma River System

River System	Sub-system	Tributary	Catchment Area (km^2)	Lahar Source
Maloma	Maloma	Maloma	99	No(*)
		Gorongoro	42	No
		Others	11	No
	TOTAL		152	

Notes: (*) previously identified as lahar source but no more unstable material is remaining.

Immediately after the eruption of Mount Pinatubo, the upper portion of the Maloma tributary was affected by pyroclastic deposits. Lahar flows were observed for several years, and a remarkable amount of lahar deposited along the river channel. Lahar flows are no longer observed although riverbed is still fluctuating in the downstream portion of the river due to floods with sediment transport.

(3) Sto. Tomas River System

The followings are tributaries of the Sto. Tomas River.

Sto. Tomas River System

River System	Sub-system	Tributary	Catchment Area (km^2)	Lahar Source
Sto. Tomas	Marella	Marella	91	Yes
	Mapanuepe	Mapanuepe	88	No
	Sto. Tomas	Santa Fe	42	No (*)
		Others	41	No
	TOTAL		262	

Notes: (*) previously identified as lahar source but no more unstable material is remaining.

The Marella River is identified as a lahar source river with a catchment area of $91km^2$ (35% of the whole catchment area of the Sto. Tomas River basin). A lake was remarkably created in 1991 by the formation of a natural dam at the confluence of the Marella and Mapanuepe Rivers due to lahar deposition from the Marella River. The Mapanuepe Lake has a surface area of $6.8km^2$ with approximately 30 million m^3 of storage capacity. The Santa Fe River was also a lahar source for several years after the eruption; however it is no longer identified as a lahar source tributary.

A topographic map produced in 1977 was compared with the recent aerial photographs taken in May 2002 to examine the changes in catchment area of the three river basins. The following table shows the changes before and after the eruption of Mount Pinatubo.

Changes in Catchment Area before and after the Eruption of Mount Pinatubo

River Basin	Catchment area before the eruption of Mount Pinatubo (1977)	Catchment area after the eruption of Mount Pinatubo (2002)	Change in catchment area
Bucao River	646 km^2	655 km^2	(+) $9km^2$
Maloma River	151 km^2	152 km^2	(+) 1 km^2
Sto. Tomas River	262 km^2	262 km^2	-

A significant change of catchment area is observed in the Bucao River basin due to the creation of the Mount Pinatubo Crater Lake as shown in Figure 1.1.7. Discharge from the Mount Pinatubo Crater Lake commenced in September 2001 at the Maraunot Notch in the Bucao River basin. The entire Crater Lake catchment area discharges to the basin.

In addition to the creation of the Crater Lake of Mount Pinatubo, many other natural lakes have been formed in the Bucao and Sto. Tomas River basins due to dams newly created at the confluence of the lahar deposition channel and its tributaries. There are 24 dammed lakes, mostly located in the Bucao River basin. Figure 1.1.8 shows the location of the dammed lakes.

1.1.6 River Channel

Channel conditions in the three rivers changed dramatically after the eruption of Mount Pinatubo due to the remarkable volume of lahar deposition along the river channels, particularly in the Bucao and Sto. Tomas Rivers.

Table 1.1.1 summarizes the major changes in the channels of the three rivers.

The volume of lahar deposition within the Bucao and Sto. Tomas River areas is estimated at 843 and 818 million m^3 respectively, as shown in Figure 1.1.7. The deposition depth is only a few meters in the lower stretches, however, the thickness increases to approximately 30 m in the upstream reaches. The huge volume of lahar deposition in the channel has significantly affected the surface run-off conditions. A

considerable volume of the surface flow infiltrates into the lahar deposition area and the surface run-off ratio is dramatically decreased particularly during flooding periods. No surface water is observed during the dry season in the Sto. Tomas River.

The area converted from riverside farm land into un-used areas due to the spread of the lahar flow along the river is estimated at 9,461 ha, of which 5,534 ha is along the Bucao and 3,797 ha is along the Sto. Tomas River stretches. The areas are currently confined by dike embankments or surrounded by mountains, and no land recovery actions have been taken.

In the lower reaches the river gradient became steeper after the eruption of Mount Pinatubo. The changes in the gradient of the lower reaches were as follows:

River Gradient in the Lower Reaches (before and after Eruption)

River	Stretch	River Length (m)		Gradient	
Bucao	Mouth ~ Malomboy	14,100	13,300	1/400	1/270
Maloma	Mouth ~ Gorongoro	7,400	7,000	1/1,200	1/800
Sto. Tomas	Mouth ~ Vega Hill	13,400	13,700	1/450	1/300
	Vega Hill ~ Mt.Bagang	13,300	12,300	1/150	1/140

1.2 Aerial Photography

1.2.1 Scope of Work

The study team used a local survey contractor, CERTEZA SURVEYING & AEROPHOTO SYSTEMS, INC to take B & W aerial photography at the scale of 1:15,000 and 1:5,000 in accordance with the specifications.

(1) Area

Aerial photographs with the scale of 1:15,000 covered top crater lake and western slope of the Mount Pinatubo and its surrounding area including the Bucao, Maloma, and Sto.Tomas River basins and the Mapanuepe Lake. Also the scale of 1:5,000 covered the Maraunot Notch and its surrounding area at the Mount Pinatubo crater.

(2) Programmed work volume and specifications

Items	First Works in the Philippines	Second Works in the Philippines
Scale	1:15,000	1:5,000
Flight Height above Ground Elevation	approximately 2,250 m	approximately 760 m
Number of Flight Lines	32 lines	1 lines
Number of Photographs	approximately 384 pcs.	4 pcs.
Photographed Area	approximately 740 km^2	approximately 0.64 km^2
Overlap	60%	60%
Sidelap	30%	30%

1.2.2 Work Execution

Clark Airport, Angeles City, Pampanga, was used as the airbase and the following equipment which met the requirements was used.

Equipment		Quantity
Aircraft	AEROCOMANDER 500U with FMS	1 unit
Aerial Camera	WILD RC-10	1 unit

For photo processing and scanning, the following equipment was used. These fully satisfied the requirements.

Equipment	Quantity
ZEISS FE-130 REWIND PROCESS EQRT.	2 UNITS
KG-30 CONTACT PRINTER	2 UNITS
ILFOLAB MG2650 PROCESSOR	1 UNIT
BESSELER FILM DRYER	1 UNIT
PHOTOSCAN TD AND A WEHRLI RM-1 SCANNER	1 UNIT

1.2.3 Output

The output of aerial photography is as follows:

Items		Set Num.	Quantity	
			1:15,000	1:5,000
Photo-Processing and Scanning	a) Contact Prints	2 sets	944 pcs	8 pcs
	b) Dia-positives	1 set	472 pcs	4 pcs
	c) Photo Scanning	1 set	472 pcs	4 pcs
	d) Photo Index Map	1 set	1 pc	1 pc
Daily Report and Flight Report		1 set	1 pc	1 pc
Quality Control Sheet		1 set	1 pc	1 pc
Camera Calibration Certificate		1 set	1 pc	1 pc

The Contractor keeps the negative films, dia-positives conforming to the laws and regulations.

The flight line and number of photographs taken with the scale of 1:15,000 are presented in Figure 1.2.1 and Table 1.2.1.

1.3 Photogrammetric/Ortho-photo Mapping

1.3.1 Scope of Work

The study team used the Japanese survey contractor, PASCO CORPORATION to make orthophoto maps and photogrammetric maps at a scale of 1:10,000 in accordance with the following specifications.

No.	Work Item		Quantity	Unit
1	Ground control survey (by GPS)		50	Stations
2	Leveling	Third Order	123	km
		Minor Order	98	km
3	Aerial Triangulation		388	models
4	Digital Mapping (1/10,000)	Orthophoto Map	300	km^2
		Photogrammetric Map	493	km^2
5	Compilation of 1:10,000		493	km^2

The ortho-photo map of 1:10,000 scale covers the top of crater lake and western slope of Mount Pinatubo and its surrounding area. The photogrammetric map of 1:10,000 scale covers the Bucao, Maloma, Sto. Tomas River basins and the Mapanuepe Lake.

Requirements of this work are tabulated below:

1	Geodetic Reference Ellipsoid		Clarke 1866	
2	Map Projection		PTM (On PRS'92)	
3	Datum of Height		Mean Sea Level	
4	Sheet size		84 cm x 59 cm (A1size)	
5	Map Scale 1:10,000		Orthophoto Map	Photogrammetric Map
6	Contour Interval	Index Contour	25 m	10 m
		Intermediate Contour	5 m	2 m
7	Required Accuracy (Standarddeviation)	Planimetry	0.3 mm on the map	
		Spot Elevation	0.5 m	
		Contour Line	1.0 m	
8	Map Style and Symbol		Provided by JICA study team	
9	Interval of Grid Ticks		1 km	

The study team used the survey contractor, CERTEZA SURVEYING & AEROPHOTO SYSTEMS, INC to make additional phtogrammetric maps at a scale of 1: 500 and topographic maps at the scale of 1:1,000 in accordance with the following specifications.

No.	Work Item	Quantity	Unit
1	Ground Control Survey (by GPS)	5	staions
2	Aerial Triangulation	3	models
3	Photogrammetric Mapping (1: 500)	0.64	km^2
4	Topographic Mapping (1: 1,000)	1.00	km^2

The photogrammetric map at the scale of 1:500 covers the Maraunot Notch and its surrounding area at the Mount Pinatubo crater. And the topographic map at the scale of 1:1,000 covers the Bucao Bridge and its surrounding area.

Requirements for additional digital mapping work are tabulated below:

1	Geodetic Reference Ellipsoid		Clarke 1866	
2	Map Projection		PTM (On PRS'92)	
3	Datum of Height		Mean Sea Level	
4	Sheet Size		84 cm x 59 cm (A1size)	
5	Map Scale		Bucao Bridge (1: 1000)	Maraunot Notch (1: 500)
6	Contour Interval	Index Contour	5 m	5 m
		Intermediate Contour	1 m	1 m
7	Required Accuracy (Standard Deviation)	Planimetry	0.3 mm on the map	
		Spot Elevation	0.3 m	0.5 m
		Contour Line	0.5 m	0.5 m
8	Map Style and Symbol		Provided by JICA study team	
9	Interval of Grid Ticks		100 m	

1.3.2 Work Specification

(1) Ground Control Survey by GPS

a) Ground control point survey shall provide the coordinates of each control point.

b) Control points were conspicuous field objects, which are identifiable on the photograph such as corners of buildings, an edge of fences or roads, etc.

c) Measurement of control points was made with the use of the existing control points.
d) The coordinates of the control points were computed based on the PTM (On PRS'92) coordinate system.
e) The Global Positioning System (GPS) was used in this survey.

f) GPS observation sessions were pre-planned such that signals from more than four satellites could be received simultaneously according to the following criteria.
- Observation was carried out simultaneously at more than three points.
- Only satellites with a vertical angle of more than 15° to 30° were observed.
- Observation times were more than one hours for more than four satellites.
- There had to be at least one redundant observation between sessions.
- Basically, the height of control points was obtained by using direct or indirect leveling of third or minor order.
- Distribution map and index maps of control points were prepared.

g) Observed points were carefully selected on the photographs and details such as location, coordinates and other information were provided in the description of pricking point.

(2) Leveling

1) Third Order Leveling

a) The elevation of benchmarks for the succeeding survey works was measured in the third order leveling.
b) Observation:
Leveling commenced from the existing NAMRIA benchmark (known point) and closed to another one. Other requirements are summarized in the table of observation standard.
c) Each measurement point established by leveling in the mapping area was identified carefully on aerial photos in the field.

2) Minor Order Leveling and Pricking

a) Minor order leveling was carried out to obtain the necessary elevation for aerial triangulation and stereo plotting.
b) Final proposed leveling route was transferred to the aerial photographs.
c) Preparation:
All important points for leveling such as road junctions, bridges, other conspicuous field objects, etc. along the leveling route were marked referring to route maps on the aerial photographs prior to commencement of work.
d) Observation:
Leveling commenced from the existing NAMRIA benchmark (known points) or new benchmarks measured by third order leveling, and closed to another one.
Other technical specifications are summarized in the table of observation standard.
e) Each measurement point by leveling was identified and marked carefully by pin-prick on the aerial photos in the field.

3) Observation Standard

Item	Third Order	Minor Order
Observation	Double Running	Single Running (In case there are no existing known points near the leveling route, double running was made.)
Given Point (Take-off or Reference Point)	Existing BM	Existing BM Third Order Leveling Point
Maximum Distance between Level and Staff	60 m	100 m
Distance between Backsight and Foresight	Balanced between Backsight and Foresight	
Minimum Unit of Measuring	1 mm	1 mm
Range of Staff Reading	The bottom 10 cm and top 10 cm of the staves was avoided	
Allowable Double Running Error	10 mm√S (S=length in km)	30 mm√S (S=length in km)
Allowable Closing Error	10 mm√S (S=length in km)	30 mm√S (S=length in km)

- Temporary benchmarks were marked on the existing permanent structures or firm and stable natural structures at approximately 5 km intervals along the leveling route.
- In case that the double running error or closing error exceeded the tolerance, re-observations were carried out.
- Field notes were submitted to the study team.

4) Check and Adjustment of Instruments

Instruments were checked and adjusted three times: before commencement of work, in the middle and at the end of work.

(3) Aerial Triangulation

On the basis of the horizontal control points and vertical control points (leveling points) indicated by the study team, the necessary photo-model coordinates of pass points and tie points for the stereo plotting were determined.

The methods were as follows:

(a) The aerial triangulation covering approx. 800 km^2 was done using high precision Digital Photogrammetric Workstation analytically.
(b) The number of models was 388. (Photo-scale: 1/15,000)
(c) A bundle method was used for the analytical aerial triangulation adjustment.
(d) The standard deviations of control points and the discrepancies of pass points and tie points between adjacent models after final adjustment were within 0.08‰ of the flying height for both horizontal and height.

(4) Digital Mapping/Digital Map-compilation

On the basis of the results of aerial triangulation and other field survey, two types of digital map data, topographic maps covering 493 km2 and ortho-photo maps covering 300 km2, were prepared separately using high precision analytical stereo plotters as follows.

(a) The plotting scale of digital map data was level 1/10,000-scale for both the topographic map and the ortho-photo map.
(b) Land-use, residential areas, main structures and annotations were included in the topographic maps.
(c) The contour intervals were 2 m in mountainous areas and 1 m intermediate contour lines in plane

areas for the topographic maps.

(d) The contour intervals for ortho-photo maps were 5 m.

(e) Digital plotted data were revised and compiled both the data and the attributes using CAD software in computers based on the field data.

(5) Ortho-photo Maps

Appling field survey data such spot heights and cross-section height data, digital contour lines created from digital elevation models, which are generated from aerial digital mapping were superimposed on the ortho-photos, and integrated as ortho-photo maps at a scale of 1/10,000.

(6) Creation of DEM

Employing the vector data of contour lines acquired with digital mapping, the DEMs (Digital Elevation Models) were generated with 20 mm cell-size in "ArcInfoGIS" software composing contour lines coverage as the three-dimensional analyzing data

(7) River Cross Section Aerial Survey

Both 1km extensions outward of riverbanks to the river cross section indicated by the study team, total length of 2 km per cross-section was implemented cross section survey.

The quantity of the work of cross section surveys was 120 in total.

Each cross section drawing was combined finally with the in river cross section data delivered by the study team.

1.3.3 Final Results

The Contractor submitted the following results to the study team

(a) Ground Control Survey

Items	Quantity	
	Proposed	Executed
Description of Pricking Point	1 set (50 stations)	1 set (50 stations)
Observation and computation results	1 set	1 set
GPS Field notes	1 set	1 set

The GPS observation networks and list of coordinates of GPS control station is shown on Figure 1.3.1 and Table 1.3.1, 1.3.2, respectively.

(b) Leveling

Items	Quantity	
	Proposed	Executed
Field note	1 set	1 set
Photo with pricked data	1 set	1 set
Information of Temporary Benchmark	1 set	1 set
Index map	1 set	1 set

The field notes and photos were kept under the custody of Contractor in the Philippines.

(c) Aerial Triangulation

Items	Quantity	
	Proposed	Executed
Computation result	1 set	1 set

(d) Digital Mapping

Items	Quantity	
	Proposed	Executed
Topo Maps (Out-putted)	1 set	1 set
Topo Map Data (CD-ROM)	1 set	1 set
Ortho-Photo Maps (Out-putted)	1 set	1 set
Ortho-Photo Map Data (CD-ROM)	1 set	1 set
Cross-section Drawings (Out-putted)	1 set	1 set
Cross-section Data (CD-ROM)	1 set	1 set

The map index sheets are shown on Figure 1.3.2.

(e) Field Completion Survey

Items	Quantity	
	Proposed	Executed
Field survey result (1/10,000)	1 set	1 set

The field surveying result was kept under the custody of Contractor in the Philippines.

(f) Additional Digital Mapping

Items	Quantity	
	Proposed	Executed
Bucao Bridge (1:1,000) Topo Maps (Out-prtted)	1 set	1 set
Bucao Bridge (1:1,000) Topo Maps (CD-ROM)	1 set	1 set
Maraunot Notch (1:500) Topo Maps (Out-prtted)	1 set	1 set
Maraunot Notch (1:500) Topo Maps (CD-ROM)	1 set	1 set

1.4 River Profile and Cross Section Survey

1.4.1 Scope of Work and Specification

The study team used the local survey contractor CERTEZA SURVEYING & AEROPHOTO SYSTEMS, INC to survey longitudinal profiles and cross-sections in accordance with the following specification.

(1) Area

The total length of river surveyed along the Bucao, Maloma and Sto. Tomas Rivers were approximately 26 km, 10 km and 24 km respectively.

(2) Leveling

Leveling to establish benchmarks for longitudinal profiling and cross section survey was third order leveling with the following accuracy.

Accuracy	10 mm$\sqrt{S}$ (S = distance in km)

(3) Longitudinal Profiling

Prior to longitudinal profiling, route surveying was carried out along the rivers. Positioning of cross sections with 1 km interval along the rivers was conducted by GPS survey and traversing. Wooden stakes (and/or equivalent) were placed at each point to identify control points for longitudinal profiling. Elevations of all stakes were surveyed by the use of levels.

The requirements of this survey are:

Accuracy	3 cm$\sqrt{S}$ (S = distance in Km)
Drawing scale	H = 1/10,000 V = 1/100
Site to be surveyed	Total distance 60 km with approximately 1 km interval

(4) Cross Sectioning

Cross section survey was carried out along the survey lines using controlled points fixed during the longitudinal profiling by measuring levels along the line.

The requirements of these survey standards are:

River name	Bucao River	Sto.Tomas River	Maloma River
Width of section (Average)	1,000 m (approx.)	1,000 m (approx.)	1,000 m (approx.)
Map scale	H = 1/5,000 V = 1/200		
Total number of sections	More than 120 sections		

1.4.2 Sounding Survey at Mapanuepe Lake

Sounding survey was executed at the Mapanuepe Lake (total length 10 km) in accordance with the following manner and accuracy:

(a) Echo sounder, GPS, sounding pole and automatic level are used.
(b) Width of sounding section in either side of the lake centerline are minimum of approximately 500 m or as directed by the study team.
(c) Height and distance of survey points on the sounding section are measured at an interval of 50 m, change of slope points, water line and lake bed.
(d) Accuracy of Sounding Survey
    a) Height error between BM and sounding section point is +/- 10 cm.
    b) Distance error between BM and sounding section is smaller than 1/300.

The requirements of the sounding survey standards are:

Like name	Mapanuepe Lake
Width of section (Average)	500 m (approx.)
Map scale	H = 1/2,000 V = 1/100
Total number of sections	13 sections

1.4.3 Establishment of Riverbed Movement Monitoring Sections

Additional river survey was conducted to analyze riverbed movement for the selected sections of the Bucao and the Sto.Tomas Rivers. A total of 14 sections (seven in the Bucao River and seven in the Sto.Tomas River) were surveyed in February 2003.

A total of 28 bench marks (one main BM and one auxiliary BM for each of the 14 cross sections) were established and marked with concrete monuments. Furthermore, a total of 14 staff gauges (seven along the Bucao and seven along the Sto.Tomas River) were established on the river bank in the vicinity of each cross section. The staffs were constructed using G.I. pipe embedded in concrete. The detailed information for the location of riverbed movement monitoring stations is described in data book in this report as a reference for further monitoring activities. The cross section data of the monitoring sections are compiled in Appendix-IV in this report as the basic data for the further assessment.

1.4.4 Survey Result

The actual amount of survey works on the longitudinal profiling and cross section surveys are summarized as follows:

River name	Bucao River	Sto.Tomas River	Maloma River
Longitudinal Profiling	26 km	24 km	10 km
Cross Sectioning	27 sections	61 sections	10 sections

Sounding survey is summarized as follows:

Like name	Mapanuepe Lake
Sounding Survey (Total Length)	10 km

Additional cross section surveys are summarized as follows:

River Name	Bucao River	Sto.Tomas River
Cross Sectioning	7 sections	7 sections

The final outputs of each survey work are:

Products	Longitudinal Profiling	Cross Sectioning
Master of Longitudinal Profiles and Cross Sections	1 set	1 set
Calculation Sheets including CD-ROM	1 set	1 set

The locations where the cross sections were measured are shown in Figure 1.4.1, 1.4.2, 1.4.3, and 1.4.4.

The final outputs of sounding survey work are:

Products	Cross Sectioning
Master of Sounding Cross Sections	1 set
Calculation Sheets including CD-ROM	1 set

The locations where the cross sections were measured are shown in Figure 1.4.5.

The final outputs of additional survey work are:

River Name	Bucao River	Sto.Tomas River
Master of Cross Sections	Calculation sheets including CD-ROM	1 set

CHAPTER 2 GEOLOGY

2.1 Geological Condition in the Study Area

Figure 2.1.1 shows a geological map of the study area. Mount Pinatubo is flanked on the west (and partly underlain) by the Zambales Ophiolite Complex. An easterly-dipping slab of eocene to pliocene marine, non-marine, and volcaniclastic sediments, namely the Tarlac Formation, is believed to unconformably overlie the Zambales Ophiolite Complex.

The Zambales Ophiolite Complex, west and northwest of Mount Pinatubo is dominantly peridotite and gabbro. North of Pinatubo is dominantly basalt.

The lower part of the Tarlac Formation is dominated by fossiliferous sandstone and siltstone, overlying the Zambales Ophiolite Complex. The upper part of the Tarlac Formation is dominated by a conglomerate, with sandstone lenses cut by andesite dikes.

The ancestral Pinatubo was an andesite and dacite stratovolcano whose center was in roughly the same location as the modern Pinatubo. Activity of the ancestral volcano ended several tens of thousands years (or more) before the caldera-forming eruption and initial growth of the modern Pinatubo.

The largest eruption in the history of modern Pinatubo occurred 35,000 years B.P., and deposited up to 100 m or more of pumiceous pyroclastic-flow material on all sides of Mount Pinatubo. These pyroclastic-flow deposits contained pumice blocks of biotite-hornblende-quartz dacite with approximately 67% SiO_2. After this eruption, the Sacobia eruptive period (17,000 years B.P.), Pasbul eruptive period (9,000 years B.P.), Crow Valley eruptive period (6,000-5,000 years B.P.), Maraunot eruptive period (3,900-2300 years B.P.), and the Buag Eruptive period (500 years B.P.) occurred prior to the 1991 eruption. The latest pre-1991 eruptive period placed pyroclastic-flow deposits in all major watersheds of Mount Pinatubo, except those of the Gumain and Porac Rivers.

2.2 Geological Investigation by Core Drilling

2.2.1 Objective and Scope of Work

The main objective of the investigation is to determine the prevailing subsoil conditions at the proposed project sites, and to obtain adequate geotechnical information relevant to the foundation design of the specific structures such as bridges and sabo/flood control facilities.

The following investigations were performed in the course of the study:

(a) Core Drilling

Fourteen core drillings were carried out at the designated bridges and river sites with Standard Penetration Tests (SPT's). The locations of each boring are shown in Figure 2.2.1 to Figure 2.2.4. The final depth, the specific location of each borehole and other information is tabulated in Table 2.2.1.

(b) Laboratory Test

All testing procedures conformed to the American Society for Testing Materials (ASTM) and the American Association of State Highway and Transportation Officials (AASHTO). Test conducted for core drillings are in Table 2.2.2. Selected samples are categorized based on Unified Soil Classification System (USCS) shown in Figure 2.2.5.

2.2.2 Result of Core Drillings

Idealized soil profiles of each site are drawn to graphically depict the subsoil conditions as revealed in the borings.

(a) Maculcol Bridge Site (Figure 2.2.6, BH-1, BH-2, & BH-3)

The results of the boreholes revealed that the project site is covered by approximately 10.0 m thick of recent lahar deposits, followed by the underlying semi-consolidated sand deposits that form the base of the boreholes.

Based on its penetration resistance (N-value) and the classification of the samples, the distinct layers as revealed by the boreholes may be categorized as follows:

Recent Lahar Deposit: This layer served as the uppermost soil cover at the project site. Based on the test results and on the visual description of the samples, this layer consists mainly of light gray medium to fine Sand and coarse to fine pyroclastics, with little amount of non-plastic fines. Classification of the selected samples falls under the SM and SP-SM category in Unified Soil Classification System (USCS).

Recorded N-values generally ranged from 12 to 25, with occasional low values from 6 to 9, and high values from 27 to 40. The recorded high N-values may be attributed to the presence of coarse pyroclastic materials that were hit during the conduct of the SPT's.

Natural moisture contents generally ranged from 15% to 17%, with sporadic high values from 25 % to 43 %. The high moisture content would indicate the presence of large amount of porous pyroclastic materials in the samples. Specific gravity test results ranged from a very low value of 2.04 to a high of 2.64, but generally ranged from 2.55 to 2.64. The very low specific gravity of 2.04 and 2.23 may be attributed to the presence of lightweight material that floats in water during the testing process.

Dense to Very Dense Sand (Older Lahar): This layer is located immediately underneath the recent lahar deposits and represents the underlying semi-consolidated granular deposits. This layer is generally described as dense to very dense, light gray to gray, coarse to fine sand, with little amount of non-plastic fines, including fine gravel and pyroclastic material. The presence of pyroclastic materials would indicate that this layer is an older lahar deposits, and probably the prevailing subsoil condition before the recent volcano eruption in 1991. This layer extended down to 26.45 m depth, the final depth of the deepest borehole, BH-2.

Recorded N-values are generally hitting practical refusals (N>50). Natural moisture contents generally ranged from 9% to 23%. Specific gravity test results ranged from 2.63 to 2.70.

Ground water table was observed at an average depth of approximately 6.0 meter in BH-1 and BH-3, reckoned from the existing ground surface elevation. In BH-2, ground water elevation is the same level as the ground surface.

(b) Maloma Bridge Site (Figure 2.2.7, BH-4, BH-5 & BH-6)

Based on the SPT N-values and the description of the samples, the prevailing subsoil condition at this project site may be categorized as follows:

Fil1 Layer: This layer served as the uppermost soil layer in BH-4 and BH-6. This fill layer consists of loose and compacted silty Sand and lahar Sand materials.

Non-plastic Silt and Clay Deposits: This layer was uncovered immediately beneath the fill layer. This layer appeared to be the upper soil layer before the fill layer in the immediate area of BH-4 and BH-6. Measured thickness is approximately 4.0 m in BH-4 and only approximately 1.0 m in BH-6.

N-values of the non-plastic silt layer ranged from a low of 3 to a high of 15, indicating very loose to

medium dense relative density. N-value of' the thin Clay layer is 3 only, indicating soft consistency.

The tests were conducted on the selected sample taken at the non-plastic silt layer yielded moisture content of approximately 32% and a specific gravity of 2.62.

Recent Lahar Deposits: This layer was encountered only in BH-5, and currently the uppermost soil deposit at the riverbed. It is generally described as very loose to loose, gray to light gray silty lahar sand with little amount of fine pyroclastics. Thickness was measured to be approximately 8.0 m.

Recorded N-values ranged from 3 to 9, with the mean of approximately 3 only.

Older Lahar Deposits: This layer was commonly encountered in the three boreholes, with thickness ranging from approximately 10.0 to 15.0 m. It was encountered beneath the silt and clay layer in BH-4 and BH-6, and immediately beneath the recent lahar deposits in BH-5.

This layer is generally described as non-plastic silty sand, with appreciable amount of gravel and coarse to fine pyroclastic materials. Color varies from grayish brown, brownish gray, and to light gray. Classification of this layer, based on the few samples, falls under the SM and ML category in USCS.

SPT results revealed that the relative density of the upper 8.0 m in BH-4 and BH-6, and the upper 4.0 m in BH-5 are medium dense ($14<N<28$), while the subsequent depths are more denser and generally hitting practical refusal ($N>50$).

Natural moisture contents ranged from approximately 35% to 45%. Specific gravity test results generally ranged from 2.51 to 2.67, with occasional low value of 2.41. As already mentioned, the low specific gravity values may be attributed to the lightweight pyroclastic materials which floats in water during the testing process.

Unconsolidated Silt/Clay and Silty/Clayey Sand Layers: These deposits were encountered beneath the very dense older lahar deposits. Thickness varies from approximately 10.0 to 12.0 m. This layer consists of inter-beds of cohesive fines and plastic/non-plastic granular deposits. The uppermost 4.0 to 5.0 m depth is overlain by the cohesive medium stiff plastic silt / silty clay, followed by the loose and non-plastic silty sand, and lastly, by the stiff to very stiff, light gray clayey Sand. Shell fragments were observed in this layer, which would suggest that this layer is a fluvial deposit.

N-values generally ranged from 4 to 15. Hydrometer tests were conducted on the fines revealed that the fines are generally silt-size (0.075 mm to 0.005 mm diameter). Natural moisture contents ranged from 22% to 34%. Specific gravity ranged from 2.55 to 2.66.

BH-4 and BH-6 were terminated in this layer at 35.45 and 30.45 m depth, respectively, reckoned from the existing ground surface elevation of the boreholes.

Silt Sand Deposit: This layer was encountered only at BH-5, beneath the unconsolidated fluvial deposits. It is described as medium dense to dense, light brown to gray, non-plastic silty Sand (SM), with traces of pyroclastic materials.

Penetration resistance was observed to be gradually increasing with depth, from an N-value of 21 to a high of 51.

BH-5 was terminated in this layer at 35.45 m depth, reckoned from the existing riverbed elevation. BH-5 is approximately 4.0 m below the top elevation of BH-4 and BH-6.

Ground water level was encountered at approximately 6.0 m depth in BH-4 and BH-6, while it is at the same level as the ground (riverbed) level in BH-5.

(c) Bucao Bridge Site (Figure 2.2.8, BH-7, BH-8 & BH-9)

The results of the boreholes revealed that the prevailing subsoil condition in BH-9 is quite distinct from BH-7 and BH-8. BH-9 is underlain by thick lahar Sand, followed by the semi-consolidated silty sand / ash layer where the borehole was terminated. On the other hand, BH-7 and BH-8 is underlain by thick unconsolidated cohesive and non-plastic sediments, and then by the underlying dunite bedrock where the two boreholes were terminated. This bedrock formation was not encountered in BH-9.

A coarse granular layer consists mainly of gravel and cobbles, however, was typically observed in all the boreholes. These distinct subsoil conditions may be further described as follows:

Subsoil Conditions in BH-7 and BH-8:

Fill Layer: This layer is composed of the upper 1.5 m thick of granular materials and by the underlying 4.0 to 5.0 m thick of cohesive soil. The upper layer of 3.0 m appeared to be a compacted fill as may be indicated by its N-value ranging from 26 to 29. On the other hand, the underlying cohesive fill described as stiff, brown silty clay is loose ($6<N<10$).

Recent Lahar Deposits: This is the current uppermost deposits at the immediate vicinity BH-8 (riverbed). This recent lahar deposits, however, was not observed/encountered at BH-7. Relative density of this recent lahar deposits is loose to very loose as indicated by its low N-values ranging from 4 to 11. The thickness is approximately 6.0 m reckoned from the existing riverbed elevation (El. +7.71 m).

Gravel/Boulders Layer: This layer was commonly observed in the three boreholes. Thickness was measured to be approximately 1.0 m only in BH-7 and approximately 4.0 m thick in BH-8. This gravel/cobbles layer appeared to be part of a man-made structure in the area prior to the recent volcano eruption. Coring procedure was utilized in advancing BH-8 into the thick gravel/cobbles layer.

Standard Penetration Tests are consistently hitting practical refusals ($N>50$).

Non-plastic Silt and Silty Clay Layer: This is the unconsolidated fines encountered beneath the gravel/cobbles layer. Thickness ranged from approximately 4.0 to 6.0 m. The upper 3.0 m of this layer is generally cohesionless in nature, and described as medium dense, brown silt (ML), with large amount of fine sand. Underneath is the cohesive fines, described as medium stiff to hard, slightly to medium plastic silty clay with little amount of sand.

N-value generally ranged from 18 to 39, with sporadic low N-value of 13 and high values of 55 and 61.

Natural moisture contents ranged from 49% to 53%, while specific gravity ranged from 2.50 to 2.63.

Sand, Gravel and silty Sand Laher: This is the granular deposits beneath the cohesive fines. In BH-7, it consists mainly of the sandy gravel material. In BH-8, this layer consists of the dense to very dense silty sand layer which in turn overlay the sandy gravel layer. N-value ranged from a low of 32 to practical refusal ($N>50$), indicating that this layer was deposited in a dense to very dense state. Classification of the sandy gravel falls under the GM category in USCS while the silty Sand layer falls under the SM category.

Natural moisture contents of the silty sand layer averaged approximately 37% while specific gravity is approximately 2.51. The sandy gravel layer has moisture content ranging from 16% to 23%, while specific gravity ranged from 2.72 to 2.78.

Dunite Boulders/Rock: This is the last layer encountered in BH-7 and BH-8, but was not encountered at BH-9. It is generally described as gray to bluish gray, moderately weathered, strongly cemented dunite. At the bottom end of BH-8, this dunite is intruded by Gabbro.

Rock Quality Designation (RQD) generally has zero values, while recovery ratio is poor to fair, ranging

from 30% to 75%.

Unconfined compression tests conducted on the selected few intact cores in BH-8, yielded unconfined compressive strength ranging from approximately 26.0 to 28.0 MPa. Average moist unit weight is approximately 28.0 kN/m^3.

Subsoil Conditions in BH-9:

Fill Layer: This fill layer consisted of the upper 3.0 m thick of medium dense silty sand, followed by the underlying 6.0 m thick of loose lahar Sand. This lahar Sand was probably a man-made fill used in the area of BH-9 during the construction of the Bridge.

N-values ranged from 14 to 21 at the upper 3.0 m depth, while it ranged from 5 to 13 at the subsequent depths.

Gravel/Boulders Layer: This typical layer in the boreholes was measured to be approximately 1.0 m thick only. Lone SPT conducted on this layer yielded N-value of 56.

Older Lahar Deposits: This thick lahar deposits was encountered beneath the gravel/cobbles layer. This layer however was unusually not encountered in the other two boreholes. Thickness of this layer was measured to be approximately 19.0 m.

This layer is generally described as light gray, medium dense, medium to coarse lahar sand, with little amount of pyroclastic materials and traces of non-plastic fines. Classification falls under SW-SM in USCS.

Natural moisture contents ranged from 15% to a high of 40%. The high moisture contents would indicate that the samples contained porous pyroclastic materials, which absorbed additional amount of moisture. Specific gravity ranged from 2.31 to 2.77. As already mentioned in the preceding discussions, the low specific gravity test results may be attributed to the presence of lightweight materials that floats in the water during the testing process.

Silty Sand Layer: This is the last layer encountered in the borehole. It consists of a semi-consolidated granular deposits described as very dense, gray silty sand, with traces of pyroclastic materials. The presence of the pyroclastic materials would indicate that this layer is a volcanic sediments or older lahar. Classification of this layer falls under SM-ML category in USCS.

Underneath this layer and was encountered at the bottom end of BH-9 is the dense, gray ash material.

Recorded N-value is consistently hitting practical refusal (N>50). Natural moisture contents ranged from 27% to 44%, while specific gravity ranged from 2.54 to 2.65.

(d) Marella River Upstream (Figure 2.2.9, BH-U1 & BH-U2)

Based on the results of the borings and referring to the idealized soil profile of this site, Figure 2.2.9, the subsoil condition at this site may be categorized into three distinct soil layers to wit:

Recent Lahar Layer: This layer served as the uppermost soil layer at the project site. It is described as loose to medium dense, light gray lahar sand, with presence of coarse and fine pyroclastic materials and little amount of non-plastic fines. Classification of this layer based on the very few samples falls under the SP-SM and SM category in USCS.

Thickness ranged from approximately 13.0 to 15.0 m. N-values generally ranged from 10 to 20. Specific gravity test conducted on this layer yielded values from 2.17 and 2.50. The low specific gravity values would indicate that the samples contain large amount of lightweight materials.

Unconsolidated Older Lahar Deposits: This layer is also described as light gray, medium dense lahar

Sand with some coarse and fine pyroclastic materials. Thin layers of' coarse pyroclastic were also observed at different depths in the boreholes. It was measured to be approximately 23.0 m thick at BH-U1 and approximately 10.0 m thick at BH-U2.

Classification of this layer falls under the SM and GP-GM category in the USCS. Plot of N-value generally falls from 20 to 35. Specific gravity ranged from 2.46 to 2.61. Natural moisture contents generally ranged from 10% to 19%.

Semi-Consolidated Older Lahar Deposits: This is the last layer encountered in the boreholes. This layer is dense to very dense, with recorded SPT N-values ranging from 30 to refusal (30<N<50). Coarse pyroclastic materials were very notable in this layer.

Classification falls under the SM and GW-GM category in USCS. This layer extended down to at least 55.45 m depth, where the deepest borehole (BH-U1) was terminated.

Natural moisture contents ranged from 14% to 17%, while specific gravity ranged from 2.53 to 2.70.

Ground water table was encountered at approximately 4.0 and 6.0 m depth reckoned from the existing ground elevation of BH-U1 and BH-U2, respectively.

(e) Marella River Downstream (Figure 2.2.10 BH-S1, BH-S2 & BH-S3)

An idealized soil profile is shown in Figure 2.2.10 to graphically depict the different soil layers encountered in the boreholes.

In general, the results of the boreholes revealed the presence of' approximately 13.0 to 21.0 m of recent lahar deposits Underneath is the older lahar deposits, then followed by the underlying bedrock. These distinct subsoil conditions are further described as follows:

Recent Lahar deposits: This layer is currently the existing uppermost soil cover at the project site. Recorded N-values at the upper 5.0 to 7.0 m ranged from 2 to 12, with mean of approximately 8 only indicating that this upper layer is loose. On the other hand, the subsequent depths have N-values ranging widely from a low of 7 to a high of 39. This wide range of N-values would probably due to the notable amount of coarse pyroclastic materials that tend to increase the penetration resistance when was hit during the conduct of SPT.

Classification of this layer generally falls under the SP-SM category in USCS. Natural moisture contents ranged from 8% to 21%, while specific gravity ranged from a low of 1.8 to a high of 2.61. Similar to the finding in the other boreholes, the very low specific gravity values would indicate the presence of large amount of lightweight materials in the samples.

Older Lahar Deposits: This layer represents the underlying unconsolidated and semi-consolidated older deposits that were probably the prevailing subsoil condition in the area of BH-S1 and BH-S2 prior to the recent volcano eruption. This layer was not encountered at BH-S3.

This layer is generally described as light gray to brownish gray, medium to fine sand, with little amount of non-plastic fines and pyroclastic materials. The upper 6.0 m thick of this layer is dense with N-values ranging from 25 to 50. In BH-S2, the bottom 6.0 m depth of this layer is very dense and consistently hitting more than 60 (N>60).

Classification of this layer based on the few selected samples falls under the SP and SM category in USCS. Natural moisture contents ranged from 15% to 23.5%. Specific gravity ranged from a low of 2.19 to a high of 2.66.

Completely Weathered Gabbro Layer: This thin layer was encountered only at BH-S3 underneath the recent lahar deposits. Thickness is approximately 1.0 meter only. This layer appeared to be the start of

the original soil cover prior to the deposition of the recent lahar. This layer served as the transition layer between the recent lahar and the underlying parent Gabbro bedrock in the area of BH-S3.

Penetration resistance (N-value) is 7, indicating medium stiff consistency. This layer is described as medium stiff, reddish brown, slightly plastic silt (ML) with some lahar sand and little amount of gravel. Natural moisture content is 36%, while specific gravity is 2.66.

Welded Tuff Bedrock Layer: This layer was detected in BH-S1 and BH-S2. It persisted down to elevation +92.7 m, the end of the deepest borehole, BH-S2. This bedrock layer was encountered at depths of 24.3 m and at approximately 37.0 m in BH-S1 and BH-S2, respectively.

This bedrock laver is described as light gray, highly to moderately weathered welded tuff. The retrieved core samples exhibits moderate to strong cementation. Coring operation was utilized in advancing into this bedrock layer. Recovery ratio ranged from 40% to a high of 100%, while Rock Quality Designation (RQD) ranged widely from zero to a high of 90%. Unconfined compression tests conducted on the intact core specimens yielded unconfined compressive strengths ranging from a low of 14.0 to a high of 28.0 MPa. Moist unit weights generally ranged from 23 to 25 kN/m^3.

Andesite Boulders/Rock Layer: This layer was detected immediately beneath the dense Sand layer in BH-S2, overlying the welded tuff bedrock layer. Thickness was measured to be approximately 2.5 m.

Gabbro Boulders/Rock Layer: This layer was detected only in BH-S3 only, where the borehole was terminated. This rock layer was encountered at 15.0m depth (El.112 m). BH-S3 was terminated at 16.0 m depth (El.110 m).

2.3 Additional Core Drilling and Laboratory Test

2.3.1 Objective and Scope of Work

The main objective of the investigation is to determine the prevailing subsoil conditions at the Bucao River dike, Sto.Tomas River dike and the Marella River, and obtain adequate geotechnical information.

2.3.2 Core Drilling

Fourteen core drillings were carried out in this study at the river dikes and river sites with Standard Penetration Tests (SPT's). The locations of each boring are shown in Figure 2.3.1 to Figure 2.3.5. The final depth, the specific location of each borehole and other information is tabulated in Table 2.3.1 and Table 2.3.2.

2.3.3 Laboratory Test

All testing procedures conformed to the American Society for Testing and Materials (ASTM) and the American Association of State Highway and Transportation Officials (AASHTO).

2.3.4 Result of Core Drilling

Subsoil conditions of each site are followed:

(a) BR-1 (Figure 2.3.6, Right Bank of the Bucao River)

The lone borehole indicated that the right bank at approximately 1.0 km downstream of the Bucao

Bridge was underlain mainly by a non-plastic recent and older lahar deposits. The recent lahar sand was measured to be approximately 18.0 m thick, while the older lahar deposit persisted down to at least 30.0 m depth (approximately El. -2.0 m).

Penetration resistance (N-value) of the recent lahar deposit ranged from a low of 3 which gradually increased to 20. The observed sudden increased in N-value (38 and 43) from 11.0 to 13.0 m depth was probably due to the presence of coarse gravel or coarse pyroclastics that were observed in the samples. N-values of the older lahar deposits ranged generally from 32 to 50.

Natural moisture content ranged 13% to 25%. Specific gravity tests results ranged from 2.61 to 2.77, with occasional low values of 2.25 and 2.54. As explained in the previous section, this low value may be attributed to the presence of lightweight materials in the sample.

Water level was detected at shallow depth of 1.0 meter near the ground surface.

(b) BR-2 (Figure 2.3.6, Crest of the Bucao River Dike)

This borehole was drilled at the crest of existing dike. The lone borehole revealed that the existing dike was made-up mainly of approximately 9.0 m high of borrow materials, consisting of mixtures of clayey sand (SC) and/or silty sand (SM-ML). N-values ranged generally from 7 to 17, with measured high blow counts of 23 and N>50 at the upper 2.0 m depth. The N-values would indicate that the dike embankment is not compacted, except the upper 2.0 m of the dike crest.

Underneath embankment (approximately El. 28.0 m) is the layer of the recent lahar deposits that persisted down to approximately 18.0 m (El. 19.0 m) depth reckoned from the existing dike crest. Measured thickness is approximately 9.0 m. Immediately beneath are the older lahar deposits that persisted down to the end of the borehole at 30.0 m.

Recorded N-values of the recent lahar deposit was observed erratic, ranging from a low of 6 to a high 25. The underlying older deposits have N-values ranging from 30 to 40, which occasional high values ranging from 42 to 50.

Natural moisture contents ranged from 14% to 29%, with occasional low values of 8% and 10%. Specific gravity tests ranged from 2.59 to 2.75.

Ground water level, measured after 24 hours, was detected at approximately 8.5 m depth, reckoned from the existing dike crest elevation.

(c) SR-1 (Figure 2.3.7, Right Bank of the Sto. Tomas River)

This lone borehole was drilled also at the existing dike crest. The borehole revealed that the upper 4.0 m of the dike was made-up of borrow soil (clayey silt and silty sand), while the bottom section of the embankment was built using lahar materials. Thickness of the lahar embankment was measured to be approximately 2.0 m.

The recent lahar deposit was distinguished from approximately 6.0 m down to 16.0 m depth, based on the observed low N-values, ranging from 3 to 10 only.

A surface deposits, described as dark gray silty clay (CL) and sandy silt (ML) was encountered immediately beneath the recent lahar at approximately 16.0 m depth. This layer appeared to be existing soil cover prior to the Mount Pinatubo eruption. Thickness of this surface deposit was measured to be approximately 4.0 m thick only, with N-values raging from 4 to 9.

Beneath this surface deposits is the older lahar deposits that persisted down to at least 30.0 m depth (El. -3.0 m), the final depth of the borehole. Measured thickness is at least 10.0 m. N-values generally ranged from 30 to N> 50.

Natural moisture contents of the surface deposits ranged from 27% to 49%, with liquid limits of approximately 44% and average plasticity index of 24%. On the other hand, the lahar deposits have moisture contents ranging generally from 11% to 14%. Specific gravity results ranged from 2.62 to 2.76, with occasional low values 2.50 and 2.58.

Ground water level was encountered at approximately 7.0 m below the present borehole elevation.

(d) SL-1-1, SL-1-2 and SL-1-3 (Figure 2.3.8, Left Bank of the Sto. Tomas River)

SL-1-1 and SL-1-3 was drilled on the riverside and landside of the existing dike, respectively, while SL-1-2 was drilled on the dike crest.

The results of the three borings indicated the presence of approximately 10 to 14 m thick of recent lahar deposits, followed by the surface deposits, and then finally by the older lahar sand deposits that persisted down to at least 30 m depth, as may be revealed by SL-1-2. SL-1-2 is the deepest borehole.

The surface deposit was measured to be approximately 4.0 m thick and was encountered starting at elevation 30.0 m in SL-1-1 and SL-1-2. On the other hand, this surface deposit was encountered only at the bottom end of SL-1-3. This surface deposit was generally described in the boring logs as gray, slightly plastic Sand and Silt mixture (SM-ML). Atterberg limit test conducted on few samples yielded liquid limit of 24% and 23%, and plasticity index of 5 and 12.

As revealed by borehole SL-1-2, underneath the surface deposit is the older lahar sand that persisted down to at least 30.0 m depth. The upper 7.0 to 8.0 m of this deposit is dense, with recorded N-values ranging between 30 and 40 m. The subsequent depth down to the end of the borehole are consistently hitting practical refusal (N>50).

Borehole SL1-2 also revealed that the existing dike embankment consisted mainly of lahar Sand materials. Thickness was measured to be approximately 5.0 m. Average N-values of the lahar embankment at the upper 2.0-m depth is 21, and 15 at subsequent depth. This confirmed that lahar embankment was not properly compacted

Natural moisture contents of lahar deposits ranged from 7% to 27%. Specific gravity test results ranged from a low of 2.52 to 2.76, but generally ranged from 2.60 t0 2.74.

Ground water level was encountered at between 37.0 and 36.0 m in the boreholes.

(e) SL-2 (Figure 2.3.9, Left Bank of the Sto. Tomas River)

This lone borehole was drilled on the dike crest. The borings uncovered approximately 5.0 m thick of lahar embankment materials. It is followed immediately by the recent lahar deposits and then by the older lahar. Similar to the other boreholes, this older lahar deposit persisted down to 30.0 m depth. Thickness of the recent lahar was measured to be approximately 13.0 m.

N-values of the lahar embankment fill ranged from 20 to 47, indicating that this layer is compacted. Recorded N-values of the recent lahar deposit generally ranged 3 to 7 only. The occasional increased in the penetration resistance in this layer was probably due to the presence of gravel or coarse pyroclastics found in the samples. The N-values at the subsequent depth (older lahar layer) were observed to quite erratic, ranging widely from a low of 10 to a high of 58. For similar reason, this quite erratic SPT results may be attributed to coarse materials that was probably hit and increased the recorded N-values.

Natural moisture contents ranged from 12% to a high of 37%. The older lahar was observed to have higher moisture contents ranging generally 31% to 37%. The unusual high moisture contents result may indicate that this layer probably contain large amount of porous materials that observed additional amount of moisture. Specific gravity tests ranged from 2.39 to 2.77. The significant numbers of low

specific gravity results (2.39 to 2.54), further corroborated the presence of porous and lightweight materials, especially in the older lahar deposits.

Ground water level was detected at approximately 8.0 m depth, reckoned from the existing dike crest.

(f) SL-3 (Figure 2.3.10, Left Bank of the Sto. Tomas River)

The result of the lone borehole drilled at the dike crest indicated that the site is underlain mainly by thick non-plastic lahar deposit. This thick lahar deposit is covered by approximately 30.0 m thick lahar embankment materials. Thickness of the recent lahar deposit in this area was measured to be approximately 14.0 m, while the older lahar deposit persisted down to approximately 40.0 m depth.

N-values of the lahar embankment is 18 on average. Similar to the other findings, the recent lahar deposits have N-values ranging from 4 to 20. On the other hand, the older lahar deposits have N-values ranging from 30 to 40, except near the bottom where the N-blows are consistently hitting practical refusal (N>50).

Natural moisture contents generally ranged from 11% to 20%, with occasional high moisture ranging 25% to 37%. Specific gravity test results ranged from 2.61 to 2.79, with low values ranging from 2.39 to 2.55.

(g) SL-4 (Figure 2.3.11, the Sto. Tomas River SL-4-1, SL-4-2, SL-4-3, SL-4-4 & SL-4-5)

The result of the five borings indicated a practically uniform subsoil conditions along the cross-section of the existing dike. The deepest borehole (SL-4-3) drilled at the crest of the dike, uncovered the thick embankment fill of approximately 14.0 m, while SL-4-2 and SL-4-4 confirmed that this fill is approximately 11.0 m thick at both sides of the existing crest (2.0 m from edge of crest). This embankment fill was made up of 4.0 to 6.0 m thick of borrow materials, while the rest was made up of lahar fill. Recorded N-values generally ranged from 10 to 30.

Beneath the embankment materials is the surface deposit, described as gray, slightly to non-plastic sandy Silt and/or silty sand (SM-ML) materials. Thickness was measured to be approximately 4.0 to 6.0 m thick in between boreholes.

The recent lahar deposits uncovered in the area of SL-4-1 and SL-4-5 was measured to be approximately 5.0 to 8.0 m thick. As revealed by SL-4-3, the older lahar deposit persisted down to 40.0 m depth. Similar to the previous findings, N-values usually ranged from approximately 10 to 20 for recent lahar, while it ranged from approximately 20 to 40 for the older lahar deposits. Similar to Sl-3, the N-values of the older lahar deposit near the bottom are consistently hitting practical refusal (N>50).

Natural moisture contents generally ranged from 10% to 20%.

Ground water level was detected at elevation 72 m to 70 m.

(h) SL-4-5 (Figure 2.3.12, Lahar filled area near the Mapanuepe Lake)

This borehole uncovered approximately 12.0 m thick of recent lahar deposits and at least 20.0 m thick of older lahar. The bore hole was terminated at 30.0 m depth. Practical refusal (N>50) was not encountered in the bore hole.

N-values of the recent lahar deposit ranged from 6 to 10 only, indicating loose relative density. On the other hand, N-values of older lahar deposit ranged from 14 to 21 only.

Natural moisture contents generally ranged from 15% to 20%, with occasional high values of 26% and 33%. Specific gravity ranged from 2.50 to 2.63.

2.3.5 Field Permeability Tests

In-situ field permeability tests were conducted at every 3-meter depth intervals. These were accomplished using the open-end (constant-head) permeability test method.

The conduct of the test is in accordance with the procedure set forth in the USBR Earth Manual.

Based on the report, Table 2.3.3 shows the results of the permeability coefficient of the following boreholes at the Sto. Tomas River dike, which ranged from 1.10×10^{-3} to 5.23×10^{-5}.

2.3.6 Field Density Tests and Relative-density Tests

Field density test was accomplished using the Sand-Cone Method (ASTMD1556). The depth of the FDT test is from 0.5 to 1.0 m.

The objectives of relative-density tests are to determine the state of density of a cohesionless deposit with respect to its maximum and minimum densities.

Based on the report, the field density and relative density are shown in Table 2.3.4.

According to the result of relative density tests, there are three types of soils. One is very high relative density and also high in-situ density (No.4), it is estimated that this soil is borrowed soil because of high density. Next soil is well compacted lahar sediment, and relative density of this soil is 6% to 14% (No.3, 5, 6). Other soils are characterized low in-situ density (No.1, 2).

2.3.7 Grain Size Analysis

The grain size analysis is an attempt to determine the relative proportions of the different grain-size which make up a given soil. And grain size distribution is necessary to distinguish the quick condition of liquefaction.

The following figure shows the possibility of quick condition of grain size distribution according to Japanese Highway Association.

This figure indicates that a lot of fine sand, grain size is from 0.8 to 0.075 mm, has a possibility of quick condition of liquefaction.

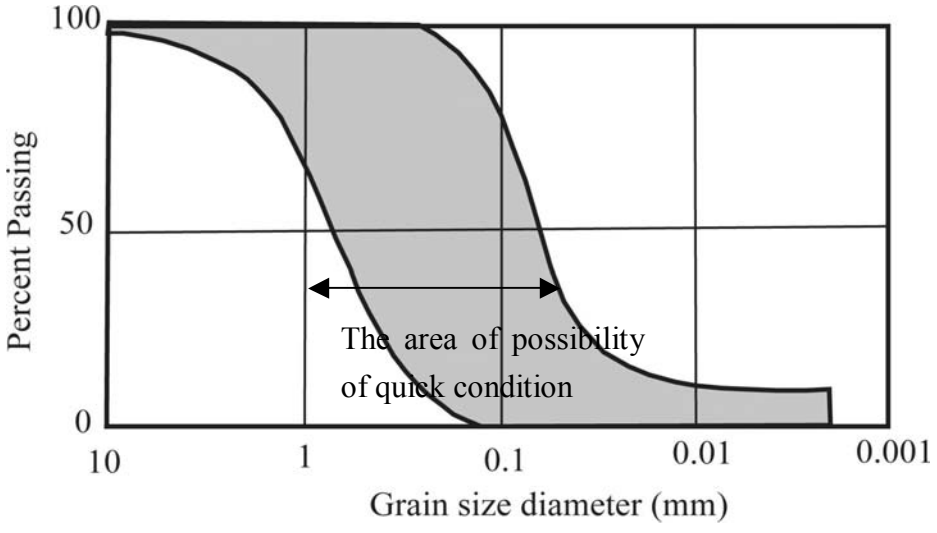

Grain Size and Possibility of Quick Condition

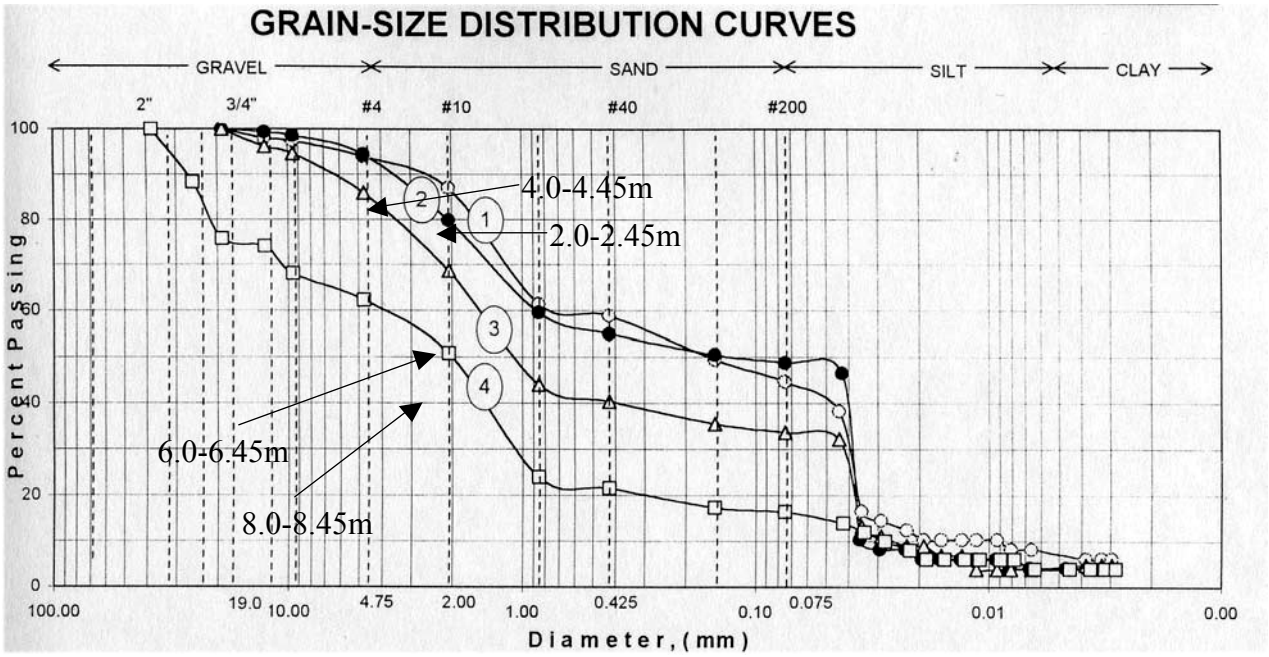

Typical Example of Grain Size Test (SL-1-2)

Based on the geotechnical report, most part of recent lahar deposits have an inclination to contain silt (grain size less than 0.075 mm), or coarse sand (grain size more than 0.8 mm). So that, almost of grain-size distribution curves of recent lahar deposits are different from this curve and are gentle curve in this grain size zone.

According to the field and laboratory test, it is concluded that the recent lahar deposits in the area of the Sto. Tomas River and the Bucao River do not have the characteristics of liquefaction.

2.3.8 Subsoil Condition of the Sto. Tomas River Dike (Figure 2.3.13)

The results of the boreholes revealed that the land side slope of the Sto. Tomas dike (STA km 17) is covered by approximately 6 to 2 m thick of borrowed soil colored reddish brown color composed of clay silt and breccia. The permeability coefficient of this borrowed soil is almost 10^{-5}, followed by the underlying embankment lahar with thickness approximately 3 to 10 m. Permeability coefficient of embankment of lahar is approximately 10^{-3} to 10^{-4} order. Following by the underlying recent lahar deposits distributed with thickness of 1.0 to 5.0 m, and permeability coefficient approximately 10^{-3}. Following by the underlying older lahar deposits developed to the bottom of boreholes.

2.4 Maraunot Notch Survey

2.4.1 Field Survey

Figure 2.4.1 presents the detailed surface geological condition around the Maraunot Notch.

The oldest geology is andesite dome which is distributed mainly along the left bank (west side) of the Maraunot Notch. The andesite, is mainly massive but locally highly jointed is unconformably overlain by fluvio-lacustrine deposit which is maybe the Crater Lake deposit and it is composed of bedded tuffaceous sandstone, siltstone and mudstone (Figure 2.4.2, Photo 9). After that, some tectonic activity occurred at the place, and then dacite lava intruded along the fault Figure 2.4.2, Photo 8, 10). Along the

fault, the dacite is strongly sheared, and with a width of approximately 10 to 20 m.

After this phenomena, some volcanic activities occurred and then breccia and lava flow deposit developed in the area (Figure 2.4.2, Photo 10,).

Subsequently, old Pinatubo volcano erupted and formed the old Crater Lake, which was similar to the present Crater Lake. And then some tufferceous sand, silt, mud and breccia deposited in the old Crater Lake (Figure 2.4.2, Photo 7).

Recent Pinatubo volcanic activity covered the mountains with some falling ash, pumice and brecci. After the eruption of Mount Pinatubo approximately 500 years ago, the Maraunot River formed on the north-west part of mountain surface.

According to the topographical map, published by NAMRIA, on a scale 1/50,000 in 1977, the Maraunot River topographically similar to the Maraunot Notch, had a gentle riverbed and wide valley (Figure 2.4.3). These topographical features indicate that the valley of the Maraunot River had been in sedimentary condition and many fluviatie sediments deposited in this valley.

Comparing the aerial photography taken in May 2002 and topography before the eruption of Mount Pinatubo in 1991, the topography indicates a small topographical change before and after the eruption in 1991 (Figure 2.4.3). This means that the sediment produced by the eruption in 1991 was not so much near the Maraunot Notch and the fundamental change of topography did not occur at the time of the 1991 eruption, only volcanic ashes covered the mountain surface. The trace of these phenomena can be seen at the down stream of the Maraunot Notch (Figure 2.4.2, Photo 2).

2.4.2 Breach of Maraunot Notch

On 10 July 2002, a huge lahar occurred along the Bucao River and carried away five carabaos and two persons, from information gathered during the field inspection. It was concluded that the occurrence of lahar was caused by the overflowing of water from the Pinatubo Crater Lake after breach of the Maraunot Notch, by comparison of photographs taken during aerial survey on 18 May (before breaching Maraunot Notch) to 18 July and 30 July (after breaching of Maraunot Notch) shown Figure 2.4.4.

Figure 2.4.5 illustrates change in topographic conditions before and after the breaching. In addition, Figure 2.4.6 shows geological condition after the breaching at the Maraunot Notch. The profile of the Maraunot River was chronologically changed due to the breach as shown in Figure 2.4.7.

A breach at the Maraunot Notch was made immediately evident by a drop in lake level distinct high water mark circumscribing crater wall. The height of water mark from the lake level was 23 m. Based on calculated lake volume released approximately 65×10^6 m^3 and the volume of lahar was estimated 160×10^6 m^3 assumption the ratios of sediment to water (3 : 2) by the PHIVOLCS.

2.4.3 Geo-resistivity Survey

The study team conducted the geo-resistivity survey around the Maraunot Notch from January 27 to February 2003 as shown in Figure 2.4.8. As a result, geologic profiles near the Maraunot Notch were obtained as shown in Figure 2.4.9 to Figure 2.4.13. The results of geo-resistivity survey were summarized is as follows:

(a) The fracturing of dacite within the sheared zone was erratic and not uniform. Within the sheared zone, the degree of fracturing tended to become higher forwards the central portions. The massive dacite as shown in the resistivity profiles may be blocky rocks within the fractured rocks.
(b) No discrete cavities or underground channels were found within the sheared zone since the variation

in resisitivity value could be correlated from resistivity station to station. Instead, the resistivity results showed that the permeability of the fractured rocks varied considerably from loose to tight.

(c) The low resistivity layers denoted highly fractured zones that were saturated with water. The interpretation of results of the geo-resistivity survey showed the absence of widened seepage zone under ground was found around the Maraunot Notch.

2.4.4 Schmidt Hammer Test

Schmidt Hammer Test was conducted at the Maraunot Notch by the study team for additional examination as shown in Figure 2.4.14. The results were as follows;

(a) Massive sandstone of fluvio-lacusrine sediment had more than 35 values of coefficient restitution of Schmidt Hammer.
(b) Sheared dacite generally had less than 15 values of coefficient restitution, but locally up to 25 to 30 values of coefficient restitution.
(c) Massive dacite mostly had 40 values of coefficient restitution.
(d) Old breccia distributed at mouth of the notch that had 22 to 30 values of coefficient restitution.

According to the result of the Schmidt Hammer Test, the sheared dacite is classified as soft rock or C_L class, the massive dacite as hard rock and C_M to C_H class, massive sandstone of fluvio-lacusrine sediment classified as hard rock and C_M class, and old breccia as hard rock or C_L class. Classification of rock is shown in Table 2.4.1

2.4.5 Probability of Future Breach

It is difficult to discuss the probability of future breach of the Maraunot Notch because of insufficient data about geological conditions and measurements on site. However, based on the results of the investigations conducted during this study and the results of the previous studies, the three scenarios for future breach might be assumed as follows.

(1) Formation of Natural Dam

Slope failure on the both right and left sides of the downstream of the Maraunot Notch would result in temporary deposition of huge amount of sediment in the river channel. The deposition may dam up the river flow and form a natural dam at the downstream of the notch. The water level at the upstream of the dam would become higher than the existing water level in the Crater Lake. Then, the collapse of the so-called natural dam will occur and deposited sediment will flow out at a burst.

(2) Seepage/Piping from Lake Water

Seepage of water of the Crater Lake may be observed somewhere at the notch or ridge of the right side. The seepage might grow gradually resulting in reducing the strength of the rock at the portion of the seepage from which collapse of the notch may occur.

(3) Shock Wave Caused by Land Slide

Once a large scale slope failure occurs inside the crater, a huge amount of sediment will fall down into the Crater Lake at a stretch, which would generate shock wave in the lake. If the shock wave floods into the notch, the portion of the notch and the ridge on the right side will be flushed away with collapse of the notch.

It is presumed that the first scenario with occurrence of slope failure at the downstream would be the most probable among the three. It can be assumed that a large scale slope failure would cause dam up of

the river because of the following reasons. First, river channel on the both sides has become steep after the collapse of the Maraunot Notch. Second, unstable deposition of volcanic ashes is observed along the long slope on the top of the river channel. Third, there is possibility of collapse of the steep slope due to erosion by the river flow. As a consequence, a natural dam might be formulated and collapse of the natural dam will cause flood in the lower reach during heavy rain.

In the case of the first scenario, breach of the natural dam would be predicted by monitoring water level at the Crater Lake or at the downstream of the Maraunot Notch because it suddenly increases during the formulation of the natural dam. The water level at the downstream of the notch can be measured by water level gauge measuring water pressure inside the borehole even when the water level is higher than the elevation of its top.

Regarding the second scenario, it is assumed that some faults might exist other than the existing fragment, which is exposed north-northwest along the river flow direction at the notch, although it can not be concluded because of uncertainty of the geology under the ground. Continuous seepage of water from the Crater Lake along such faults would reduce the strength of rocks in the long term. When the water level at the Crater Lake suddenly rises due to heavy rain, the water will be flushed away from the crater with collapse of the notch portion and ridge on the right side due to high water pressure. In this case, such collapse will not occur soon because it takes long time until the strength of the rock becomes critically weak as seepage grows gently.

With respect to the third scenario, slopes inside the crater have not been stable yet with continuous small-scale slope failure. In future, it is possible that the water in the Crater Lake may overflow at the ridge on the right side of the notch with collapse if shock wave caused by direct fall of the mass into the lake attacks the notch. It can not be concluded that the third scenario would be realized because of the uncertainty of the conditions of geology and failure of the slope inside the crater.

2.4.6 Proposed Countermeasures

Now, the mechanism of the breach of the Maraunot Notch is estimated like above description, the condition of the Maraunot Notch is different from the one in September 2002 not only topographically but geologically. Almost non-consolidated deposits have been washed away, and the surface of ground are covered with consolidated materials like as old breccia, intrusive dacite and fluvio-lacoste deposits. Therefore, it seems that such large-scale breach may not occur as the breach in July 2002. This is different from the conclusion as of September 2002.

Tables

Table 1.1.1 Changes in River Channel before and after Eruption of Mount Pinatubo

River System	Stretch	River Length (m)		Gradient		Average Bed Elevation (Lower End)		Average Bed Elevation (Upper End)		River Area (ha)		Lahar Deposit Volume (mil.m3)	
		1977	2002	1977	2002	1977	2002	1977	2002	1977	2002	1977	2002
Bucao	Mouth ~ Bucao Bridge	3,000	2,600	1/470	1/500	0.0	0.4	4.9	5.0	91	217	-	1
	BucaoBridge ~ Baquilan	7,600	7,300	1/330	1/260	4.9	5.0	24.7	30.0	860	1,454	-	65
	Baquilan ~ Malomboy	3,500	3,400	1/340	1/190	24.7	30.0	35.4	49.2	300	710	-	53
	Upper Bucao	23,100	22,700	1/90	1/90	39.3	49.8	271.7	285.9	1,160	3,288	-	400
	Balin Baquero	24,200	21,300	1/80	1/100	31.5	48.6	300.0	260.6	699	2,975	-	324
	TOTAL									3,110	8,644		843
Maloma	Mouth ~ Maloma Bridge	2,600	2,400	-	1/800	0	0.8	-	3.8	29	44	-	1
	Maloma Bridge ~ Maloma / Gorongoro Confluence	4,800	4,600		1/800	-	3.8	-	8.9	58	173	-	2
	TOTAL									87	217		3
Sto. Tomas	Mouth ~ Maculcol Bridge	1,600	1,400	1/400	1/580	0	2.2	3.6	4.7	61	151	-	1
	Maculcol Bridge ~ Umaya	7,700	7,800	1/580	1/340	3.6	4.7	16.1	26.2	305	449	-	30
	Umaya ~ Vega Hill	4,100	4,500	1/300	1/240	16.1	26.2	29.7	43.1	184	510	-	68
	Vega Hill ~ Mt.Bagang	13,300	12,300	1/130	1/130	29.7	43.1	110.5	129.6	303	2,610	-	390
	Marella River	7,100	6,800	1/50	1/60	110.5	129.6	233.5	232.8	56	794	-	260
	Mapanuepe River	13,700	11,500	1/320	1/1,800	110.5	129.6	129.6	132.9	113	305	-	69
	TOTAL									1,022	4,819		818

Source: JICA Study Team

Table 1.2.1 Photo Course and Quantity

The list of 1:15,000 Scale Aerial Photos

Line NO.	Photo NO.	Quantity
Line 1	5639-5654	16
Line 2	5672-5655	18
Line 3	5453-5478	26
Line 4	5207-5226, 5503-5496	28
Line 5	5253-5231, 5504-5508	28
Line 6	5254-5278, 5510-5509	27
Line 7	5303-5279, 5511-5512	27
Line 8	5304-5329	26
Line 9A	5856-5854, 5352-5341, 5521-5516	21
Line 9B	5340-5330, 5515-5513	14
Line 10A	5355-5369	15
Line 10B	5370-5378, 5528-5530, 5381	13
Line 11A	5402-5394	9
Line 11B	5542-5531	12
Line 12A	5679-5673	7
Line 12B	5543-5554	12
Line 13A	5680-5685	6
Line 13B	5567-5555	13
Line 14A	5690-5685	5
Line 14B	5568-5580	13
Line 15A	5794-5788	7
Line 15B	5599-5581	19
Line 16A	5795-5800	6
Line 16B	5600-5619	20
Line 17A	5808-5801	8
Line 17B	5627-5622, 5436-5424, 5621-5620	21
Line 18A	5809-5817	9
Line 18B	5628-5634	7
Line 19A	5830-5818	13
Line 20	5831-5843	13
Line 21	5850-5844	7
Line 22	5405-5410	6
	Total =	472

Table 1.3.1 GPS Coordinates

Station	*Northing*	*Easting*
G 2	1,687,838.601	428,837.459
G 3	1,673,372.304	427,836.036
G 4 **(KE22)**	1,686,957.823	427,161.357
G 5	1,672,088.571	426,008.692
G 6	1,688,049.646	423,987.304
G 7	1,680,955.582	421,266.748
G 8	1,663,098.184	422,809.386
G 9	1,666,405.541	420,884.133
G 10	1,657,740.951	421,297.847
G 11	1,688,534.162	419,629.884
G 12	1,685,376.966	417,840.347
G 13	1,666,347.998	417,593.161
G 14	1,662,941.500	417,345.079
G 15	1,656,845.778	417,059.606
G 16	1,651,015.424	417,091.680
G 17	1,686,849.616	415,553.164
G 18	1,682,197.330	415,650.908
G 19	1,660,624.344	415,378.354
G 20	1,652,141.860	413,470.335
G 21	1,684,689.707	413,494.339
G 22	1,689,596.907	411,296.063
G 23	1,656,469.228	411,214.493
G 24	1,688,579.207	409,107.414
G 25	1,660,527.690	408,531.050
G 26	1,688,663.023	406,876.948
G 27	1,653,590.975	406,874.980
G 28 **(KE7)**	1,689,580.355	404,637.972
G 29	1,664,769.201	404,658.888
G 30	1,688,212.308	403,111.571
G 31 **(KE5)**	1,653,425.959	402,562.873
G 32	1,692,335.430	400,475.099
G 33	1,671,237.236	400,617.878
G 35	1,653,832.487	398,693.391
G 36	1,692,886.704	398,244.477
G 37	1,695,442.110	396,083.387
G 38	1,688,074.922	395,716.425
G 39	1,698,050.607	394,189.627
G 40	1,686,147.571	393,888.119
G 41	1,693,701.341	392,163.443
G 42	1,698,225.391	389,799.198
G 43	1,694,938.816	390,261.366
G 44	1,698,874.527	388,164.103
G 45	1,675,185.696	398,013.886
G 46	1,674,245.193	402,791.979
G 47	1,668,184.680	398,800.947
G 48	1,649,438.984	408,796.234
G 49	1,648,375.137	413,216.008
G 50	1,655,721.624	423,610.536
G 51	1,655,231.864	425,907.653
Z BS 1	**1,704,522.814**	**387,411.849**
Z BS 2	**1,658,463.796**	**405,279.987**
Z BS 5 **(G34)**	1,660,797.581	399,343.837

Table 1.3.2 Elevation of GPS, BM, Pricking Points (1/3)

Elevation List of Used GPS points, Benchmarks and Pricking points

NAME	ELEVATION	NAME	ELEVATION	NAME	ELEVATION
ZA29A	40.246	TBML1	4.221	TBMD1	7.736
ZA35A	40.678	TBML2	4.024	TBMD2	5.603
ZA38A	35.294	TBML3	4.518	TBMD3	(=B19)
ZA46A	9.535	TBML4	4.452	TBMD4	8.279
ZA47A	9.195	TBML5	10.932	TBMD5	19.442
ZA54	7.298	TBML6	4.044	TBMD6	36.756
ZA56A	7.570	TBML7	5.777	TBMD7	69.260
ZA58A	8.718	TBML8	6.323	B1	6.790
ZA61A	6.393	TBML9	35.113	B2	7.023
ZA62A	4.352	TBML10	43.901	B3	9.137
ZA66A	6.338	TBML11	44.451	B4	10.306
ZA68A	4.674	TBML12	39.222	B5	12.735
ZA73A	4.102	L1	4.221	B6	16.193
ZA82A	4.853	L2	3.014	B7	5.238
ZA91A	6.078	L3	2.499	B8	5.765
ZA93A	3.620	L4	3.240	B9	6.547
ZA94	5.375	L5	4.097	B10	7.626
ZA97A	3.935	L6	3.858	B11	6.910
ZA111A	3.962	L7	3.632	B12	8.156
BMNAR2	4.325	L8	4.690	B13	9.180
G2	362.9	L9	5.636	B14	10.073
G3	970.7	L10	6.409	B15	10.647
G4 (KE22)	428.219	L11	7.636	B16	11.218
G5	760.4	L12	10.417	B17	6.368
G6	275.164	L13	11.084	B18	5.583
G7	322.2	L14	12.097	B19	4.360
G8	208.969	L15	18.626	B20	3.476
G9	309.487	L16	8.934	B21	4.791
G10	126.767	L17	8.989	B22	6.283
G11	194.963	L18	9.726	B23	6.925
G12	158.829	L19	8.554	B24	8.130
G13	160.283	L20	9.359	B25	7.198
G14	106.508	L21	11.242	B26	9.267
G15	100.511	L22	11.049	B27	10.028
G16	46.086	L23	12.114	B28	11.421
G17	124.365	L24	12.745	B29	11.912
G18	167.229	L25	4.405	B30	11.796
G19	76.033	L26	4.962	B31	11.734
G20	45.850	L27	3.945	B32	12.326
G21	123.824	L28	3.651	B33	13.124
G22	73.280	L29	4.332	B34	14.249
G23	46.834	L30	4.061	B35	15.608
G24	63.018	L31	4.654	B36	15.556
G25	48.579	L32	5.177	B37	17.542
G26	51.749	L33	4.896	B38	19.612
G27	21.684	L34	5.537	B39	14.571
G28 (KE7)	45.342	L35	3.655	B40	15.491
G29	16.321	L36	4.208	B41	18.469
G30	34.936	L37	6.092	B42	22.456
G31	9.927	L38	6.111	B43	22.954

Table 1.3.2 Elevation of GPS, BM, Pricking Points (2/3)

NAME	ELEVATION	NAME	ELEVATION	NAME	ELEVATION
G32 (KE5)	21.030	L39	6.909	B44	28.579
G33	9.460	L40	7.515	B45	28.563
G34 (ZBS5)	7.440	L41	7.152	B46	25.702
G35	2.661	L42	7.421	B47	29.281
G36	15.128	L43	7.308	B48	33.207
G37	11.823	L44	7.687	B49	13.451
G38	4.928	L45	8.479	B50	16.324
G39	12.758	L46	10.707	B51	15.509
G40	4.109	L47	18.689	B52	16.990
G41	5.561	L48	14.586	B53	19.396
G42	4.211	L49	6.519	B54	19.825
G43	4.859	L50	6.191	B55	27.777
G44	3.872	L51	4.840	B56	28.828
G45	6.074	L52	5.431	B57	66.609
G46	65.504	L53	6.796	B58	66.293
G47	4.696	L54	5.747	B59	71.730
G48	24.604	L55	5.478	B60	33.541
G49	32.711	L56	6.049	B61	34.419
G50	276.766	L57	5.943	B62	35.730
G51	160.002	L58	5.887	B63	37.813
KE3	8.073	L59	6.401	B64	39.946
KE6	20.763	L60	5.814	B65	41.452
SM100	161.032	L61	4.761	B66	24.435
SM101	179.575	L62	4.564	B67	25.330
SM102	295.509	L63	4.817	B68	27.430
SM103	296.758	L64	4.576	B69	30.094
SM104	277.527	L65	4.218	B70	31.471
SM105	270.787	L66	4.772	B71	33.209
SM106	230.024	L67	5.359	B72	35.174
SM107	238.466	L68	13.450	B73	37.149
SM108	238.346	L69	7.980		
SM109	234.339	L70	6.424		
SM110	197.265	L71	6.562	L113	3.219
SM111	144.396	L72	5.433	L114	43.004
SM112	134.207	L73	7.071	L115	41.597
SM113	137.863	L74	8.336	L116	43.884
SM114	136.030	L75	10.078	L117	44.643
SM115	146.899	L76	3.621	L118	43.614
SM116	156.050	L77	4.130	L119	43.427
SM117	165.456	L78	5.384	L120	44.657
SM118	179.346	L79	5.394	L121	46.594
SM119	191.073	L80	5.552	L122	46.711
SM120	126.955	L81	5.826	L123	46.137
SM121	123.745	L82	4.201	L124	43.234
SM122	115.389	L83	5.232	L125	44.898
SM123	107.696	L84	4.173	L126	41.514
SM124	100.885	L85	3.322	L127	41.067
SM125	96.467	L86	36.780	L128	40.046
SF1	101.984	L87	38.521	L129	57.475
SF2	95.064	L88	41.064	L130	71.654
SF3	90.443	L89	42.006	L131	74.360
SF4	81.949	L90	44.775	L132	75.978

Table 1.3.2 Elevation of GPS, BM, Pricking Points (3/3)

NAME	ELEVATION	NAME	ELEVATION	NAME	ELEVATION
SF5	77.389	L91	48.117	L133	81.932
SF6	77.803	L92	49.971	L134	86.700
SF7	76.473	L93	51.631	L135	90.135
SF10	177.077	L94	54.008	L136	44.019
SF11	165.754	L95	6.347	L137	44.007
SF12	170.080	L96	6.729	L138	43.777
SF13	179.388	L97	6.094	L139	42.986
SF14	196.474	L98	6.439	L140	42.097
SF15	212.149	L99	8.129	L141	39.333
SF16	227.175	L100	9.791	L142	36.914
SF17	252.292	L101	20.077	L143	34.174
SF18	265.260	L102	21.573	L144	32.228
SF19	343.207	L103	19.482	L145	28.843
SF20	340.452	L104	5.372	L146	28.648
SF22	240.643	L105	9.273	L147	27.437
SF23	253.691	L106	5.634	L148	26.772
SF24	253.394	L107	NONE	L149	26.083
SF25	182.334	L108	8.097		
SF26	150.868	L109	6.961		
RT1	40.846	L110	6.016		
RT2	64.619	L111	5.251		
RT3	86.947	L112	3.885		
RT4	67.575	BT1	325.658		
RT5	121.258	BT2	318.925		
RT6	67.119	BT3	290.490		
RT7	168.366	BT4	247.982		
RT8	140.613	BT5	230.863		
RT9	130.101	BT6	210.520		
RT10	124.896	BT7	204.980		
RT11	117.753	BT8	189.581		
RT12	93.791	BT9	175.402		
RT13	84.098	BT10	158.347		
RT14	74.484	BT11	150.508		
RT15	74.407	BT12	143.224		
RT16	80.398	BT13	130.223		
RT17	66.056	BT14	119.920		
RT18	66.483	BT15	114.618		
RT19	63.357	BT16	119.535		
RT20	53.532	BT17	123.514		
RT21	62.549	BT18	124.960		
RT22	46.268	BT19	125.942		
RT23	38.828	BT20	130.076		
		BT21	133.314		
		BT22	142.610		
		BT23	165.140		

Table 2.2.1 Details of Core Drillings

Name of Bridge/River	Borehole ID.	Relative Location	Depth (m)	Number of Penetration Test
Maculcol Bridge	BH-1	Left Bank	40	40
	BH-2	Center of River	40	40
	BH-3	Right Bank	40	40
Maloma Bridge	BH-4	Left Bank	30	30
	BH-5	Center of River	35	35
	BH-6	Right Bank	30	30
Bucao Bridge	BH-7	Left Bank	20	20
	BH-8	Center of River	40	40
	BH-9	Right Bank	35	35
Marella-U1	BH-U1	Left Bank	30	30
Marella-U2	BH-U2	Left Bank	30	30
S1	BH-S1	Left Bank	20	20
S2	BH-S2	Left Bank	35	35
S3	BH-S3	Center of River	20	20
Total	14 Boreholes		445.0	

Table 2.2.2 Tests Conducted for Core Drillings

ASTM Designation	Title / Description
1. D2488	Visual-Manual Classification of Soils.
2. D2487	Classification of Soils for Engineering Purposes.
3. D2216	Water (Moisture) Content of Soil, Rock, and Soil-Aggregate Mixtures.
4. D422	Particle size Analysis of Soils.
5. D2938	Unconfined Compressive Strength of Intact Rock Core Speciments.
6. D854	Specific Gravity of Soil Solids.

Table 2.3.1 Additional Core Drillings

Name of River	Borehole ID.	Relative Location	Depth (m)	Number of Penetration Test
Bucao River	BR-1	Right Bank	30	30
	BR-2	Right Bank	30	30
Santo Toms River	SR-1	Right Bank	30	30
	SL-1-1	Left Bank	15	15
	SL-1-2	Left Bank	30	30
	SL1-3	Left Bank	15	15
	SL-2	Left Bank	30	30
	SL-3	Left Bank	40	40
	SL-4-1	Left Bank	10	10
	SL-4-2	Left Bank	20	20
	SL-4-3	Left Bank	40	40
	SL-4-4	Left Bank	30	30
	SL-4-5	Left Bank	15	15
Marella River	SL-5	Center of River	30	30
Total	14 boreholes		365	

Table 2.3.2 Tests Conducted for Additional Core Drilling

ASTM Designation	Title / Description
1. D2488	Visual-Manual Classification of Soils
2. D2487	Classification of Soils for Engineering Purposes
3. D2216	Water (Moisture) Content of Soil, Rock, and Soil-Aggregate Mixtures
4. D422	Particle size Analysis of Soils
5. D854	Specific Gravity of Soil Solids
6. D2049	Relative-Density Determination

Table 2.3.3 Results of Permeability Tests

BOREHOLE ID	PERMEABILITY	
	DEPTHS (m)	COEFFICIENT, K
SL 4 -1	3	5.20 × 10-3
SL 4 - 2	3	5.59 × 10-3
	6	3.55 × 10-3
	9	3.75 × 10-4
SL 4 - 3	6	1.56 × 10-4
	9	1.49 × 10-3
	12	4.59 × 10-4
	15	5.23 × 10-5
	18	1.10 × 10-3
	21	3.60 × 10-4
SL 4 - 4	3	7.88 × 10-5
	6	4.67 × 10-4
	9	2.56 × 10-3
	12	1.25 × 10-3
SL 4 - 5	3	3.15 × 10-3

Table 2.3.4 Results of Field Density and Relative Density Test

Sample number	Borehole Number	Location	Depth (m)	Laboratory Dry Density Test		In-Situ Dry Density	Natural Moisture Content	Relative Density
				Maximum Density	Minimum Density	G/cc	%	%
1	SL-1	River Side	0.0-0.5	1.23	1.00	1.00	28.86	57.83
		2.0 m. from Dike Crest (Land Side)	0.0-0.5	-	-	-	-	-
2		Land Side	0.0-0.5	1.79	1.59	1.13	3.53	16.36
3	SL-4	River Side	0.0-0.5	1.72	1.47	1.50	6.37	9.91
4		2.0 m. from Dike Crest (Land Side)	0.0-0.5	1.84	1.52	1.75	5.71	71.90
5		Land Side	0.0-1.0	1.68	1.39	1.43	11.93	13.61
	BR-2	Land Side	0.0-0.5	-	-	1.38	42.79	-
		2.0 m. from Dike Crest (River Side)	0.0-0.5	-	-	1.48	16.58	-
6		River Side	0.0-0.5	1.71	1.44	1.46	5.06	6.04

Table 2.4.1 Classification of Rock for Schmidt Hammer Test

Symbol of classification			Tanaka's classification	Uniaxial Strenghth ($kg \cdot f/cm^2$)	Velocity of transversal wave (m/s)	Geology: Example of rock name	Geology: Type of rock: Igneous rock	Geology: Type of rock: Volcanic sedimentary rock	Geology: Type of rock: Metamorphic rock	Geology: Type of rock: Sedimentary rock	Geology: Geologic times	Indication of rock quality: R.O.D (%)	Indication of rock quality: Reaction coeffient of Schmidt hammer	Indication of rock quality: Velocity of longitudinal wave (km/s)
Hard rock H	H_1	A～B	A～B	>1000	2,000～3,000	Andesite Granite Slate Shale Tuff Sundstoe etc.	(Oligocene)				Before Paleogene Tertiary	100	45～	5.0
	H_2	C_H	C_H	800<	1,800～2,500							100	40～	4.0～5.0
	H_3	C_M	C_M	400～500	1,200～1,800							50～90	35～	3.0～4.0
	H_4	C_L	C_M C_L	300～400	700～1,500		(Miocene)				(23MY)	20～80	25～	2.5～3.5
Soft rock S	S_1	D_H	C_L	100～300	500～1,300	Shale Mudston Sundstone Tuff Siltstone Weathered mudstone etc.	(1) Newly sedimentary rock (2) Igneous sedimentary rock (3) Weathered granite				Neogene Tertiary		15～	1.5～2.5
	S_2	D_M	D	50～100	400～900									<1.5
	S_3	D_L		20～30<	300～700		(Polocene)							<1.2
	S_4	E		5～10<	200～500									
Diluvium gravel	Boulder (>30cm)				400		(Diluvium) Gravel				(1.8MY)			
	Cobble (>7.5cm)				300									
	Gravel (>0.2cm)				200～300									
Soil materials	Sand			5～10	200～300						Quaternary			
	Silt			2～5	150～200		(Holocene)							
	Clay			1～2 0.5	100～50 50～100		Alluvium							